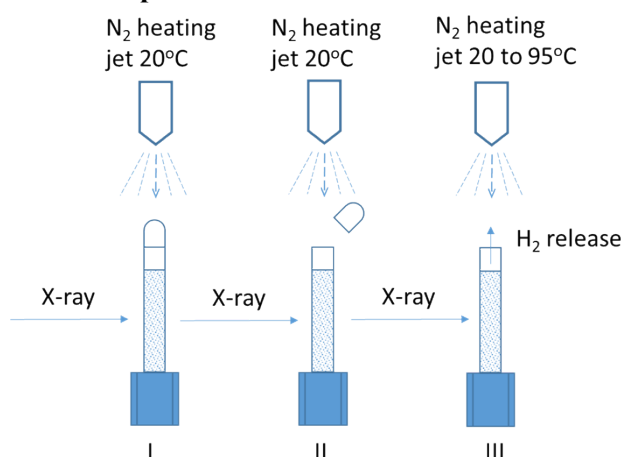**Electronic Supplementary Information (ESI)**

1. Experimental

Scheme S1. The experimental setup used for in-situ XRD measurements

Scheme S1 shows the experimental procedure for in-situ XRD measurements.

I. Sample packed in a sealed XRD 0.5mm borosilicate glass capillary (Prepared in Glove box)

II. Cap of capillary is removed under N_2 heating jet at $20^{\circ}C$

III. Sample decomposition under N_2 heating jet from 20 to $95^{\circ}C$ with a heating rate of 2 $^{\circ}C$ min^{-1}.

2. Low energy mechanical milling effects on AB

Thermal decomposition of pure AB after milling for 5, 10, 15, 30, 60 and 120 mins at a relatively low ball to powder ratio of 10 to 1 was first studied to clarify the milling effect. As shown in Fig. S1, mechanical milling under the current milling conditions does not alter the decomposition properties of AB, including dehydrogenation temperature, kinetics, mass loss and volatile gas emissions. As shown in the MS profiles, volatile products, NH_3, $N_3B_3H_6$ and B_2H_6, mainly come from the second decomposition step, which shows much more mass loss than that from the first one. Comparison of the XRD patterns and the NMR measurements of the samples ball milled for different periods of time, Fig S2 indicates that there was no AB phase change and decomposition under the current milling conditions, while the prolonged high-energy ball milling over 2 hours may result in local overheat which leads to the melting and decomposition of AB.
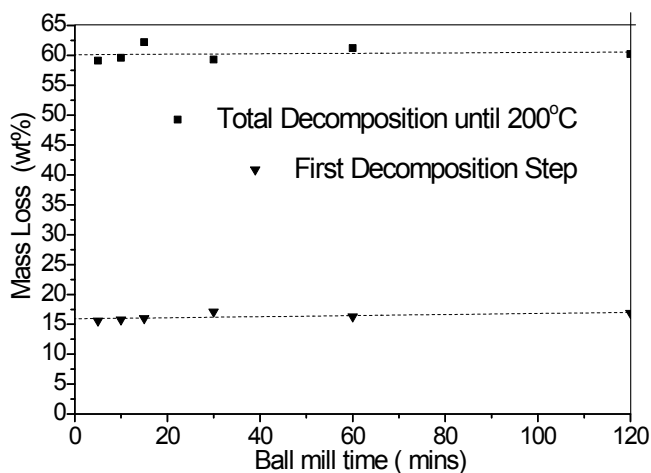
Figure S1 (a) The mass loss evolution of the first decomposition step and the whole reaction until 200 ºC of the AB as the function of the milling time.
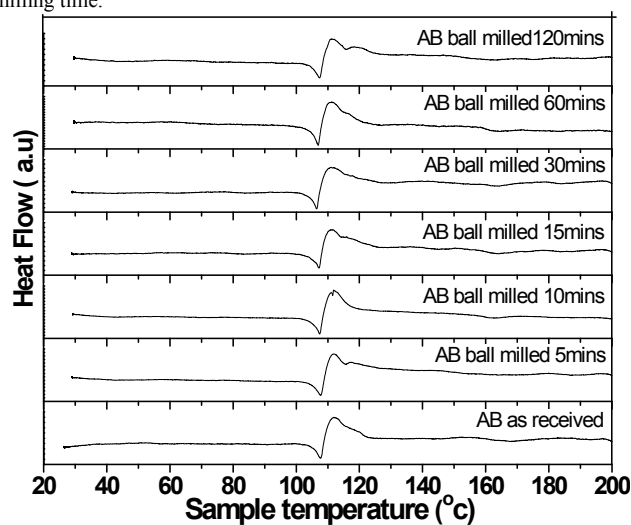

Figure S1(b) DTA curves comparison as the function of the temperature for the pure AB ball milled for 0,5,10,15,30,60,120 mins, measured by DTA under flowing Argon, with a heating rate of 2ºC/min.
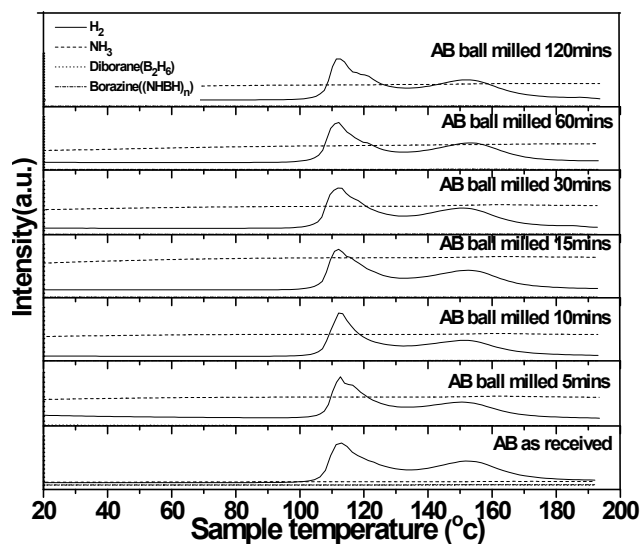

Figure S1(c) MS profiles as the function of the temperature for the pure AB ball milled for 0, 5,10,15,30,60,120 mins, measured under flowing Argon, with a heating rate of 2ºC/min
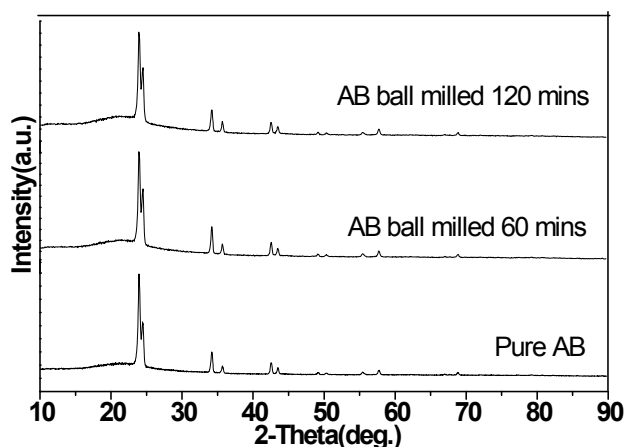
Figure S2 (a) Evolution of XRD patterns of the AB after different periods of ball milling.
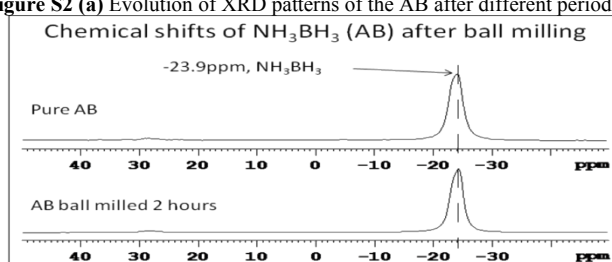

Figure S2 (b) ^{11}B MAS NMR spectra of the AB after different periods of ball milling.

The phase evolution and chemical shifts of AB during thermal decomposition are shown in Figs. S3 and S4. The conditions of the thermal decomposition in in-situ XRD and NMR were similar to that in TG/DTA/MS measurement, the heating rate was controlled as 2 °C/min, and the samples were under protection of N_2 inert gas flow. In the case of XRD, the phase evolutions were recorded every 5 °C, while in NMR measurements, the spectra were taken every 4 °C to 55 °C, then every 2 °C to 97 °C, the samples were maintained at 97 °C for 12 mins, the spectra were taken every 2mins. The XRD result shows that a continuous peak shift of AB towards the low-angle side with increasing temperature, particularly after 60 °C, which should be due to the distortion of the AB lattice. Moreover, the intensity of the AB starts to decline at 80°C, and has significant decrease after 100 °C, where the distinct peak disappearance is observed and the sample turns to an amorphous feature. It corresponds to the temperature of melting and decomposition of the AB.
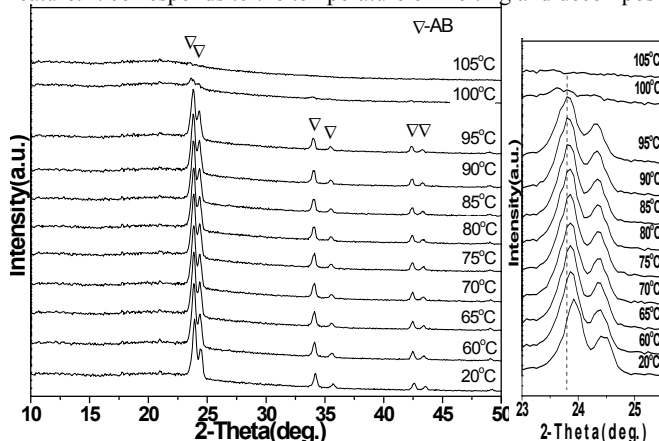

Figure S3 *In-situ* Evolution of XRD patterns of the as-received pure AB during the heat treatment under N_2 until 105°C(left), with enlarged angle range (2θ = ca.23° -25.5°)(right), heating rate was set as 2°C/min.
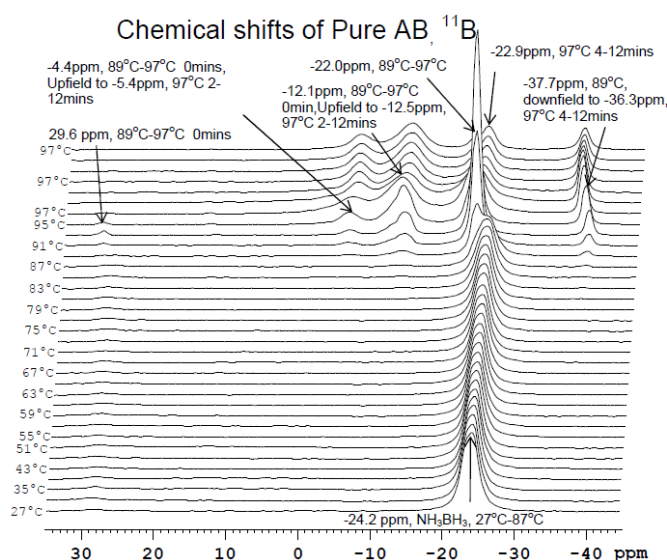
Figure S4 *In- situ* ^{11}B MAS NMR spectra of the decomposition of Pure AB upon 97°C, heating rate 2 °C/min

The 11B NMR study gives a further insight into the physical and chemical transformations of AB during the thermal decomposition. As shown in Fig. S4, pure AB shows BH_3 with chemical shift of - 24.1 ppm, which is in agreement with previous published NMR data on AB [6]. With increasing temperature, AB undergoes gradual degradation up to 89 °C, where a significant transformation occurs. New borane species with chemical shift of -22.3, -12.1, -4.1 and -37.7 ppm are observed simultaneously from ~ 89 to 97°C, which correspond to $BH_3(N)$, $BH_2(N_2)$, $BH(N_3)$, and BH_4 species, respectively. Moreover, a quick resonance at 29.2 ppm is observed from 89 to 97 °C and it should be associated with sp2 borane in the polyborazylene. It is noted that subtle shifts are observed in most of the species along with the further increase of temperature. The BH_4 species downfield shifts to -36.3 ppm, at 4 mins after the temperature reaches 97 °C. While $BH(N_3)$ and $BH_2(N_2)$ species upfield shifts to -5.4 and -12.4 ppm, respectively. The BH3(N) species with a chemical shift of -22.3 ppm is consistent with previous finding of a new AB mobile phase [6], which is referred to as AB*. This new AB phase undergoes similar transformation here; it rapidly gains the maximum intensity at 93 °C and subsequently degrades but still can be identified at the end. However, very complex chemical shift is observed on this BH3(N) species, it downfield shifts to -21.9 ppm at 2 mins after the temperature reaches 97 °C. Then a new resonance turns up at -22.6 ppm, it subsequently upfield shifts to -22.9 ppm at 4 mins after the temperature reaches 97 °C, then it broadens and becomes featureless. The NMR findings in our experiment are in agreement with previous NMR studies from the literature very well [6], except the new peak at -22.9 ppm.

As the dehydrogenation of AB is likely to involve intermolecular interactions, so if the mobility of the reaction species increases, the reaction rate will be considerably enhanced. The in-situ NMR results (see Fig.S4) show that a new mobile AB phase is formed before hydrogen release, which could result from the disruption of the dihydrogen bond network. The disruption of the dihydrogen bond network leads to enhanced mobility of the AB molecule, which favours subsequent AB-AB intermolecular interaction and hydrogen release with a considerable enhanced reaction rate. However, the new mobile AB phase still exhibits a similar crystal structure to AB, but with an expanded lattice, as shown in the in-situ XRD in Fig. S3. Concurrent with the appearance of the AB mobile phase, the presence of BH_2 and BH_4 species indicate the formation of Diammoniate of Diborane (DADB), $[BH_2(NH_3)_2][BH_4]$, and this observation is consistent with a previous report, by Tom Autrey et al [6], where it is proposed that the early-stage decomposition of AB involved solid-state nucleation and growth, which shows exothermic features and results in the formation of a mobile AB phase and DADB. These products are of similar crystal structure to AB. Our studies agree very well with their NMR findings and also confirm the decomposition of AB through their proposed pathways: 1) Induction: disruption of dihydrogen bonding, formation of a new AB mobile phase. 2) Nucleation: formation of DADB. 3) Growth: reaction of DADB with AB. However, the new chemical species at -22.9 ppm was not observed in their study, probably due to different reaction temperatures involved in the studies. The high reaction temperature 97 °C (88 °C used in their study) may lead to further transformation, where a new $BH_3(N)$ species with a higher electron density around of the borane centre is formed. Furthermore, there is no mobile AB phase observed in the sample during the different periods of ball milling, which suggests that the dihydrogen bond network can be disrupted in the heat treatment process only, rather than ball milling under current conditions. The NMR results also indicate the presence of BH (N_3) and sp^2 borane, which strongly suggests that the AB also undergoes cyclotriborazane decomposition to borazine and further decomposition to polyborazylene. This side cross-link reaction occurs concurrently with the AB poly-pyrolysis

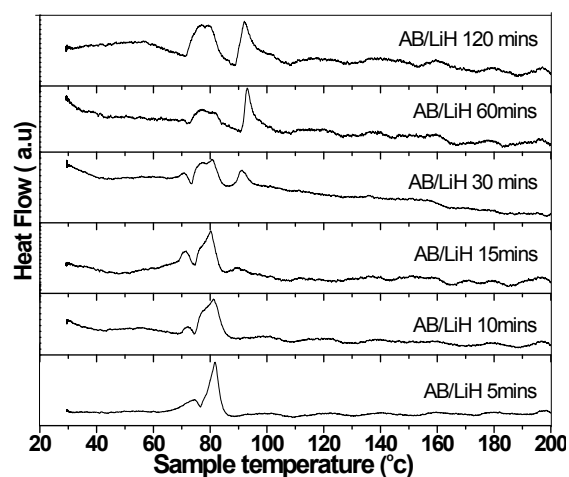## 3. Low energy mechanical milling effects on (AB+LiH) systems

Figure S5 (a) DTA curves as the function of the temperature for the AB/LiH ball milled for 5,10,15,30,60,120 mins, measured under flowing Argon, with a heating rate of 2 º C/min.
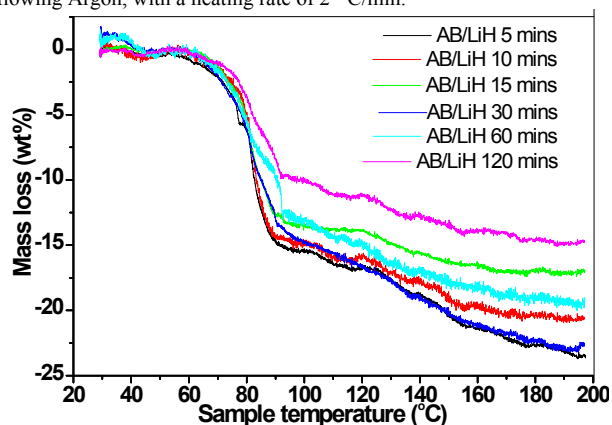

Figure S5 (b) Amount of dehydrogenated hydrogen (wt %) as the function of the temperature for the AB/LiH ball milled for 5, 10, 15, 30, 60, 120 mins, measured under flowing Argon, with a heating rate of 2 º C/min.
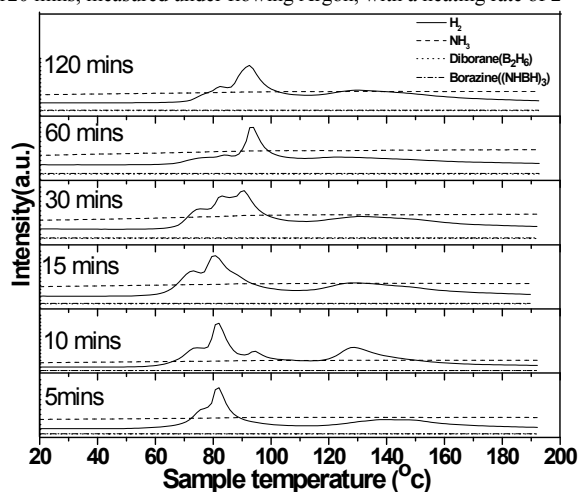

Figure S5 (c) MS profiles as the function of the temperature for the AB/LiH ball milled for 5,10,15,30,60,120 mins, measured under flowing Argon, with a heating rate of 2 ºC/min.
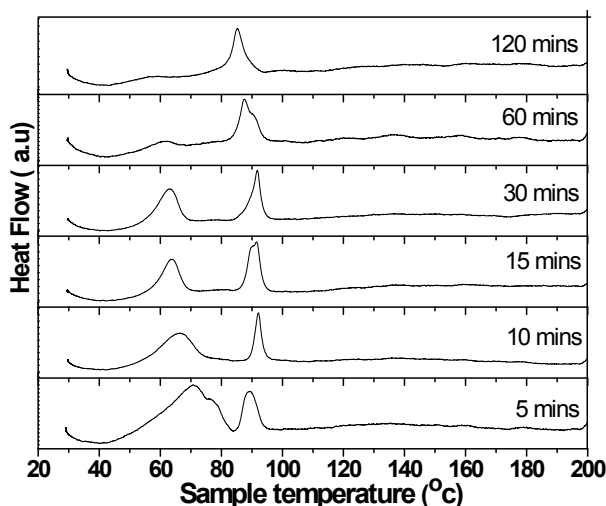
Figure S6 (a) DTA curves as the function of the temperature for the 3AB/5LiH ball milled for 5, 10, 15, 30, 60 and 120 mins, measured under flowing Argon, with a heating rate of 2 º C/min.

Figure S6 (b) Amount of dehydrogenated hydrogen (wt %) as the function of the temperature for the 3AB/5LiH ball milled for 5, 10, 15, 30, 60 and 120 mins, measured under flowing Argon, with a heating rate of 2 º C/min.
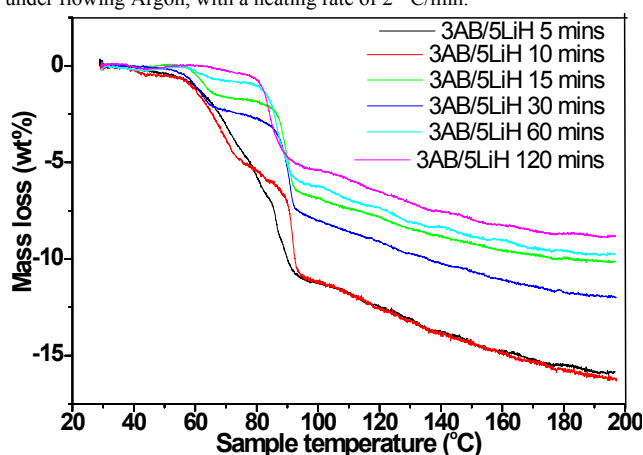

Figure S6 (c) MS profiles as the function of the temperature for the 3AB/5LiH ball milled for 5, 10, 15, 30, 60 and 120 mins, measured under flowing Argon, with a heating rate of 2 º C/min

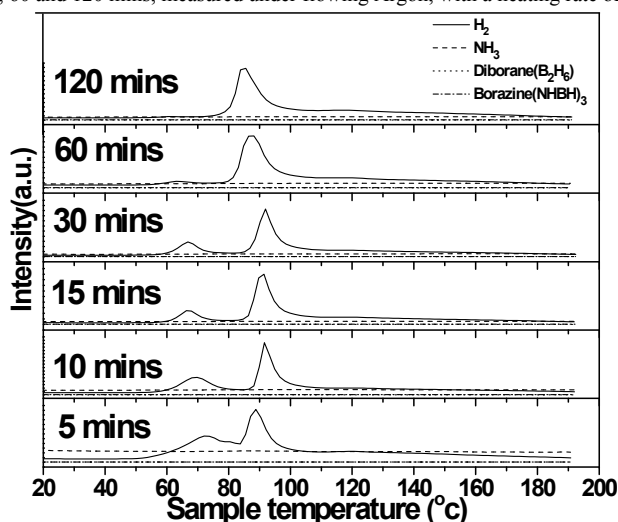The area under the DTA (which is a more accurate term for our system than DSC; the term has been corrected throughout) curve could be used to indicate the exothermicity of the reaction between (AB+LiH), but quantitative analysis will require another type of facility (DSC). Generally speaking, the extent of exothermicity reduces with increasing milling time, due to the reduced amounts of AB and LiH, accompanied by the increasing level of the intermediate phase. However, comparing the results of dehydrogenation temperature and capacity, the specimen milled for 10 mins is more desirable, with a balanced reduction of dehydrogenation temperature and high capacity. And this exothermic trend co-relates with the total hydrogen release, as now shown in Figure S6 (b).
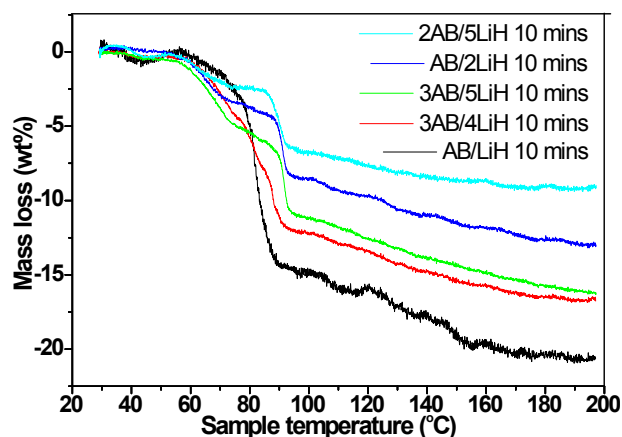
Figure S7 Amount of dehydrogenated hydrogen (wt %) as the function of AB:LiH molar ratio of 1/1, 3/4, 3/5, 1/2 and 2/5, measured under flowing Argon, with a heating rate of 2ºC/min.
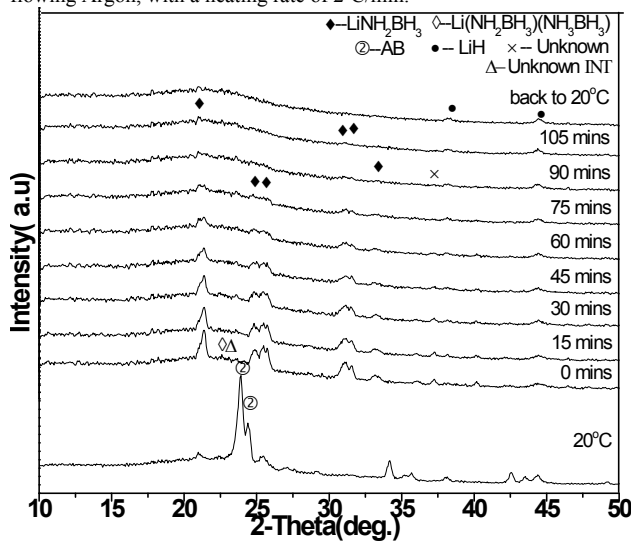

Figure S8 (a) *In-situ* Evolution of XRD patterns of the 10mins ball milled 3AB/5LiH composition during the isothermal heat treatment under N_2 until 85ºC, heating rate 30ºC/min.
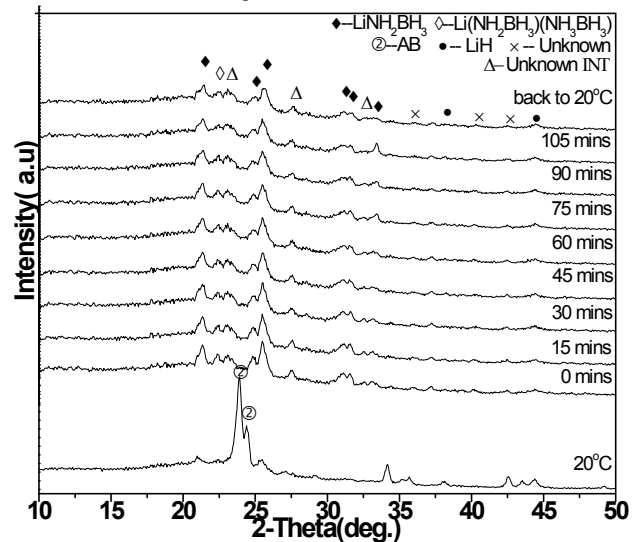

Figure S8 (b) *In-situ* Evolution of XRD patterns of the 10mins ball milled 3AB/5LiH composition during the isothermal heat treatment under N_2 until 75ºC, heating rate 30ºC/min.

4. Further modification of AB/LiH systems

In our further efforts to optimize the dehydrogenation properties of the AB/LiH systems, particularly the 3AB/5LiH samples, different modifications on the milling conditions and additives were carried out, including pre-milling AB for 2, 3 and 4 hours, and short time shaking of the AB/LiH mixture. Pre-milling AB to a certain extent gives advantage of refining the AB particles in advance thus increasing the surface contact between AB and LiH in subsequent milling. While, shaking involves less input energy and avoids further hydrogen release. As shown in Fig 15. Pre-milled AB does not show any significant improvement on the dehydrogenation properties. It strongly suggests that the reaction kinetics of AB and LiH relies on the surface reaction, where the mobility of the reaction species plays a more import role in the reaction, rather than diffusion which is strongly affected by particle size. It is also worth mentioning that the shaked 3AB/5LiH mixture even shows worse dehydrogenation property. It has similar DTA profile to the 10 mins-ball-mixed AB/LiH mixture but its XRD pattern shows the absence of $LiNH_2BH_3$, $LiNH_2BH_3 \cdot NH_3BH_3$ and the unknown intermediate phase. The results are in contrast to the findings in ball-mixed samples. It implies that the reaction of AB and LiH has not been initiated during the shaking process, or not to a critical extent. This probably due to the insufficient mixing and less impact energy and friction involved by milling balls. The comparative observations seem to suggest that a small extend of milling is necessary, e.g. to introduce surface defects and to initiate a low-level of reaction between the AB and LiH, which can be considered as *in-situ* "product seeding", to generate a small amount of $LiNH_2BH_3$, $LiNH_2BH_3 \cdot NH_3BH_3$ and the unknown intermediate phase as nucleation sites for subsequent dehydrogenation reaction. The "product seeding" has been shown to lower the activation energy barrier by seeding diammoniate of diborane for the dehydrogenation of AB [39]
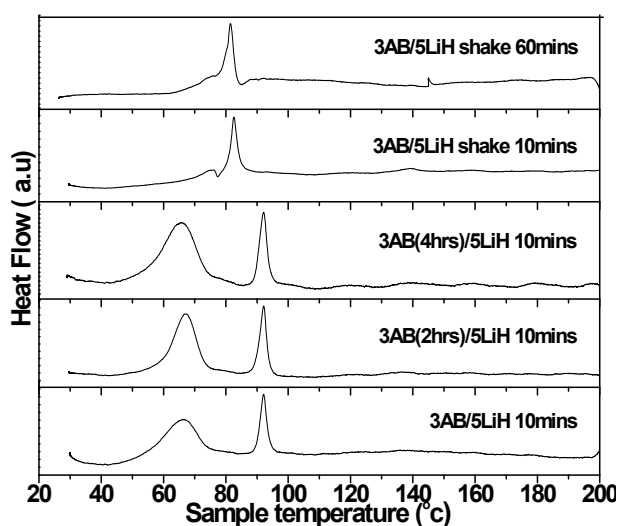

Figure S9 (a) DTA curves as the function of the temperature for the10mins ball milled and shaked mixture of the 3AB/5LiH, AB were pre-milled at different time of 2, 3, 4hrs in advance, measured by DTA under flowing Argon, with a heating rate of 2ºC/min.
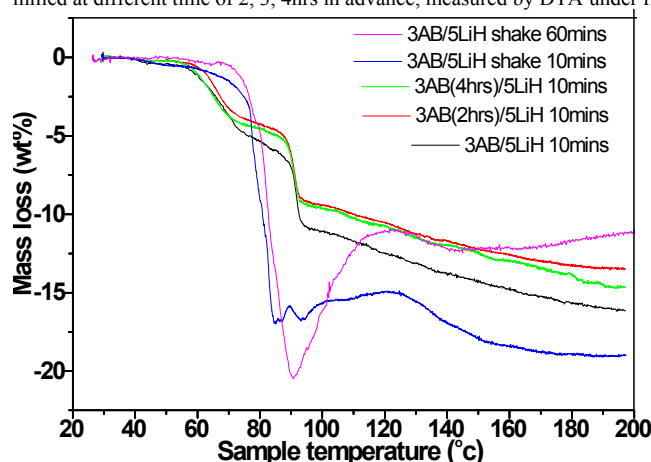

Figure S9 (b) Mass loss as the function of the temperature for the10mins ball milled and shaked mixture of the 3AB/5LiH , AB were pre-milled at different time of 2, 3, 4hrs in advance, measured by TG under flowing Argon, with a heating rate of 2ºC/min
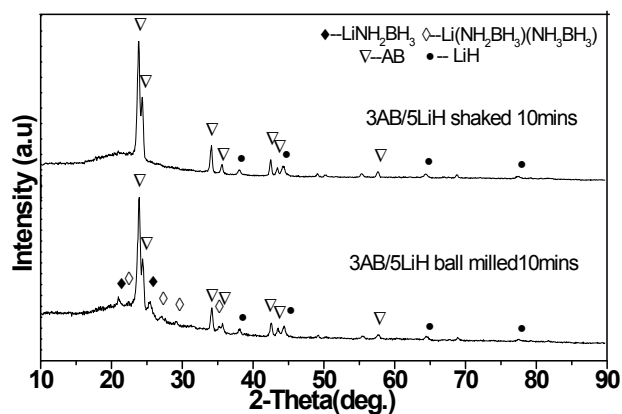
Figure S9 (c) XRD patterns of 3AB/5LiH composition under 10mins ball milled and 10mins shaked (no milling balls)

In our further effort to promote the dehydrogenation properties of AB+LiH mixture, different types of chemical additives have been employed and studied. As shown in Fig S5 in supplementary information. Graphite cannot readily interact with AB and LiH in a short period of ball milling, but it does offer contribution to refine the particle of host material and reduce adhesion and agglomeration [40]. Here, the addition of graphite does not improve the dehydrogenation properties of AB+LiH systems; this also indicates that the reaction kinetics replies on surface reaction, rather than diffusion. Thus the particle refinement is not that important in this case.

The replacement of the H in the N of AB by alkali metal, i.e Li, leads to the transfer of dihydrogen bond stabilized molecular crystal AB to ionic crystal compound $LiNH_2BH_3$, which has remarkable improvement on the dehydrogenation properties, compared to pure AB. Doping ionic compound LiCl into AB and LiH systems can increase the ionicity of the mixture, and thus enhances the reaction of AB and LiH to a certain extent during the ball mixing.
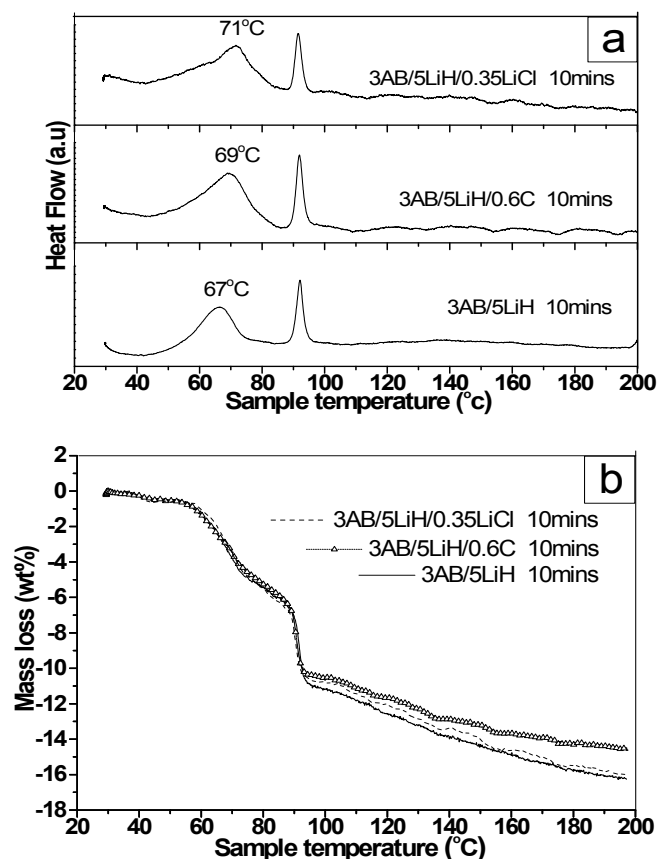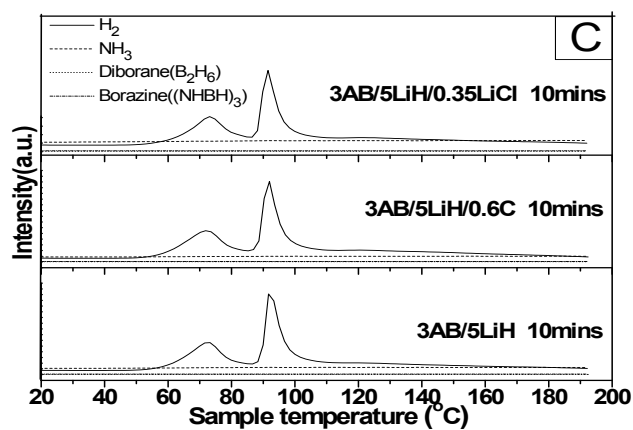
Figure S10 Comparison of the a) DTA curves; b) Amount of dehydrogenated hydrogen (wt %); c) MS curve as the function of the temperature for the 3AB/5LiH(70/30) and 3AB/5LiH/0.6C, 3AB/5LiH/0.35LiCl, measured under flowing Argon, with a heating rate of 2ºC/min

References

1. A. C. Stowe, W. J. Shaw, J. C. Linehan, B. Schmid and T. Autrey, *Phys. Chem. Chem. Phys.*, 2007, **9**(15), 1831–1836.

2. C. X. Shang and Z. X. Guo, *J. Power Sources*, 2004, **129**(1), 73–80.

3. Y. H. Hu and E. Ruckenstein, *J. Phys. Chem. A*, 2003, **107**(46), 9739–9741.